Quantum Entangled Images

A. Gatti, E. Brambilla, and L. A. Lugiato
Dipartimento di Fisica, INFM, Via Celoria 16, 20133 Milano, Italy

M. I. Kolobov
Fachbereich Physik, Universität-GH Essen, D-45117 Essen, Germany
(Received 12 October 1998)

We analyze a scheme consisting of an optical parametric amplifier and two imaging lenses. From an off-axis input image such a system creates two *quantum entangled* output images, signal and idler, symmetrical with respect to the optical axis of the scheme. In the limit of large amplification the idler image is a quantum twin of the signal one in the sense that they display identical intensity fluctuations in space-time.

PACS numbers: 42.50.Dv, 03.67.–a, 42.65.–k

The possibility of quantum correlations (entanglement) between light beams played a major role in the recent development of quantum optics. It is now clear that entanglement, an ubiquitous and intriguing concept in quantum physics, represents an opportunity because it leads to novel applications such as quantum cryptography, quantum computation, and quantum teleportation. Entanglement phenomena in optics have been investigated, however, recently at the level of single photon pairs (see, e.g., [1]) and in the temporal domain. The demonstration of spatial aspects of quantum entanglement in light for systems with a large number of photons may increase substantially the amount of information involved in applications. Starting from our investigation on the quantum aspects of optical pattern [2], in this paper we predict the possibility of generating pairs of optical images that are quantum entangled to each other. This result may pave the way to the development of a quantum optics of images, intended to explore how quantum features could be used in the parallel processing of information.

Recently we analyzed the spatial correlations of intensity fluctuations in the far field of the light emitted by a degenerate optical parametric oscillator (OPO) with spherical mirrors below threshold. We considered the total number of photons N_1 and N_2 in two regions of the far-field plane, symmetrical with respect to the optical axis of the system, and showed that the fluctuations in the difference $N_- = N_1 - N_2$ are largely below the shot-noise level [3].

While in the case of [3] the emitted light arises from the amplification of vacuum fluctuations, in this article we address a situation where the radiation field carries information, because it corresponds to the amplification of an image. As a result of our analysis we predict the phenomenon depicted in Fig. 1. The element OPA/OPO corresponds to a cavityless optical parametric amplifier (OPA) or to an OPO with planar mirrors below threshold [4]. We consider type I, nearly degenerate phase matching in the nonlinear crystal. Not shown in the figure is the plane-wave pump field of frequency ω_p, activating the parametric down-conversion process; L and L' are imaging lenses. An input image I is injected in the OPA/OPO at the frequency $\omega_p/2$; at the output one has an amplified version I_S (signal image) of the input, plus the phase-conjugate image I_I (idler image). In the limit of large amplification, signal and idler images have the same mean intensity distribution. We demonstrate that in the same limit these two images are quantum mechanically entangled; I_I and I_S are correlated much better than two classical copies because the intensity fluctuations in each portion of I_I are "identical" to those in the corresponding portion of I_S. Precisely, the fluctuations in the intensity difference are well below the shot noise level.

Before discussing the scheme in Fig. 1, let us consider the simpler situation shown in Fig. 2, in which there are no lenses and we focus our attention on two plane waves at the frequency $\omega_p/2$, symmetrically tilted with respect to the system axis. Namely, if $\vec{x} \equiv (x, y)$ is the position vector in any transverse plane, and $\vec{k} \equiv (k_x, k_y)$ is the transverse component of the wave vector, we consider two plane waves of the form $e^{i\vec{k}\cdot\vec{x}}$ and $e^{-i\vec{k}\cdot\vec{x}}$. Indicating by $a^{\text{in}}_{\vec{k}}$ and $a^{\text{in}}_{-\vec{k}}$ the annihilation operators of photons for the input waves and $a^{\text{out}}_{\vec{k}}$, $a^{\text{out}}_{-\vec{k}}$ those for the output waves, they are linked by a unitary transformation of the form

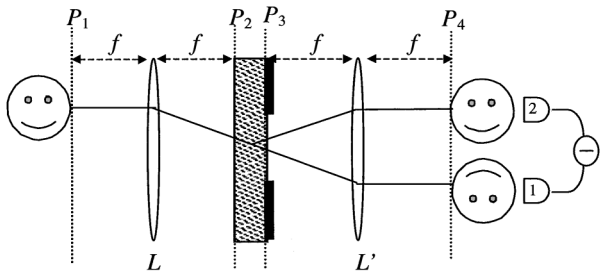

FIG. 1. Parametric image amplifier in the phase-insensitive configuration: the object is confined to the upper half of plane P_1; the two-lens system allows for projection of the amplified signal and idler images in plane P_4.

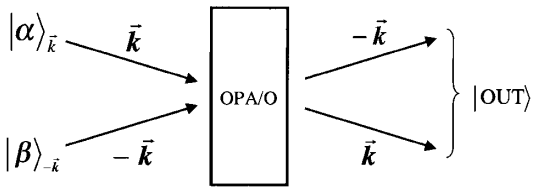

FIG. 2. Schematic representation of an OPA/OPO with two tilted input waves in the coherent states $|\alpha\rangle_{\vec{k}}$ and $|\beta\rangle_{-\vec{k}}$; amplification is phase insensitive for $\alpha \neq 0$, $\beta = 0$, and phase sensitive for $\alpha = \beta \neq 0$.

(see, e.g., [5,6])

$$a_{\vec{k}}^{\mathrm{out}} = e^{i\psi}[\cosh(r)a_{\vec{k}}^{\mathrm{in}} + e^{i\phi}\sinh(r)a_{-\vec{k}}^{\mathrm{in}\dagger}], \tag{1a}$$

$$a_{-\vec{k}}^{\mathrm{out}} = e^{i\psi}[\cosh(r)a_{-\vec{k}}^{\mathrm{in}} + e^{i\phi}\sinh(r)a_{\vec{k}}^{\mathrm{in}\dagger}]. \tag{1b}$$

We assume that the two input waves are in coherent states $|\alpha\rangle_{\vec{k}}$ and $|\beta\rangle_{-\vec{k}}$, respectively. By applying the transformation (1a) and (1b) on the state, rather than on the operators, the uncorrelated input state $|\alpha\rangle_{\vec{k}}|\beta\rangle_{-\vec{k}}$ is transformed into the entangled output state of the two waves [7]

$$|\mathrm{OUT}\rangle = G(\psi)\exp\{\zeta a_{\vec{k}}^{\dagger}a_{-\vec{k}}^{\dagger} - \zeta^{*}a_{\vec{k}}a_{-\vec{k}}\}|\alpha\rangle_{\vec{k}}|\beta\rangle_{-\vec{k}}, \tag{2}$$

where $G(\psi) = \exp[i\psi(a_{\vec{k}}^{\dagger}a_{\vec{k}} + a_{-\vec{k}}^{\dagger}a_{-\vec{k}})]$, and $\zeta = re^{i\phi}$. Let us distinguish two cases: (a) The input wave $-\vec{k}$ is in the vacuum state, i.e., $\beta = 0$, with $\alpha \neq 0$. The wave $\vec{k}$ undergoes phase-insensitive amplification, with $\cosh(r)^2$ being the intensity amplification factor. In the output the ratio of the intensity of the wave $-\vec{k}$ to that of wave $\vec{k}$ is $\sinh(r)^2/\cosh(r)^2$ and tends to unity when $\cosh(r)^2 \gg 1$. This situation was analyzed theoretically and experimentally by Kumar *et al.* in [8], as an extension of their previous work [9] to the spatial domain. They demonstrated that the intensity difference between such two waves exhibits fluctuations below the shot-noise level. (b) The two input waves have the same amplitude, $\beta = \alpha$, so that the input field has a spatial distribution of the form $\cos(\vec{k}\cdot\vec{x})$. When recast in terms of the waves $\cos(\vec{k}\cdot\vec{x})$ and $\sin(\vec{k}\cdot\vec{x})$, the model (1a) and (1b) describes two independent single-mode degenerate parametric amplifiers, so that the waves experience phase-sensitive amplification. Such a case is equivalent to that analyzed theoretically and experimentally in temporal domain by Levenson *et al.* [10], using polarization degrees of freedom instead of spatial modes. In the output, two waves have highly correlated quantum fluctuations in the amplified quadrature components.

In our device (Fig. 1) we consider the amplification of an image instead of a plane wave, with a phase-insensitive amplification as described in the case (a). Essential elements in our scheme are the imaging lenses L and L' (see Fig. 1) first introduced in [6]. The analysis of [6], however, was focused on phase-sensitive amplification and did not consider the quantities relevant here.

We designate by $a_1(\vec{x},t)$, $a_2(\vec{x},t)$, $a_3(\vec{x},t)$, $a_4(\vec{x},t)$ the slowly varying (with respect to the carrier frequency $\omega_p/2$) operators in the input plane P_1, the entrance plane of the amplifier P_2, the exit plane of the amplifier P_3, and the output plane P_4, respectively. We denote by $a_i(\vec{x},\Omega)$, $a_i(\vec{k},\Omega)$ $(i = 1,\ldots,4)$ their Fourier transforms in time, and in space-time.

By neglecting a pump depletion, the fields $a_3(\vec{k},\Omega)$ and $a_2(\vec{k},\Omega)$ are related by the following input-output transformation:

$$a_3(\vec{k},\Omega) = u(|\vec{k}|,\Omega)a_2(\vec{k},\Omega) + v(|\vec{k}|,\Omega)a_2^{\dagger}(-\vec{k},-\Omega), \tag{3}$$

where, compared to Eqs. (1a) and (1b), we have included the temporal arguments. The explicit form of the functions $u(|\vec{k}|,\Omega)$ and $v(|\vec{k}|,\Omega)$ can be found in [5] for the OPA and in [6] for the OPO. For an OPA they depend on the phase mismatch along the propagation direction, the dispersion relation in the crystal, and the parametric gain [5]; for an OPO they are functions of the cavity detuning, its decay constant, and the distance from oscillation threshold of the OPO [6]. For our purposes, however, only relevant is the unitarity condition $|u(|\vec{k}|,\Omega)|^2 - |v(|\vec{k}|,\Omega)|^2 = 1$.

The lenses L and L' located as shown in Fig. 1 map the Fourier plane (k_x,k_y) into the physical plane (x,y), so that the system amplifies a portion of the image instead of a band of k vectors. In the absence of the pupil A, operators in the input and the output planes are related by the following transformation, valid in the paraxial approximation:

$$a_4(\vec{x},\Omega) = -\overline{u}(|\vec{x}|,\Omega)a_1(-\vec{x},\Omega) + \overline{v}(|\vec{x}|,\Omega)a_1^{\dagger}(\vec{x},-\Omega), \tag{4}$$

where

$$\overline{u}(|\vec{x}|,\Omega) = u\left(\frac{2\pi|\vec{x}|}{\lambda f},\Omega\right),$$
$$\overline{v}(|\vec{x}|,\Omega) = v\left(\frac{2\pi|\vec{x}|}{\lambda f},\Omega\right), \tag{5}$$

λ is the wavelength of the signal field, and f is the focal length of the lenses. The pupil A introduces into relation (4) a convolution [11] with the *impulse response function* of the system [6]. The pupil area S_A determines the resolution area S_R of the scheme, $S_R = (\lambda f)^2/S_A$.

The region of optimal amplification is characterized by the spatial scale x_0 of variation of the functions $\overline{u}$, $\overline{v}$ [5,6],

$$x_0 = \frac{f\lambda}{2\pi}\Delta k, \quad \text{with } \Delta k = \sqrt{2\pi/\lambda l_{\mathrm{eff}}}, \tag{6}$$

where l_{eff} is the crystal length for the OPA, and $l_{\mathrm{eff}} = L/T$ for the OPO, with L being the cavity length and

T the transmission coefficient of the coupling mirror; Δk represents the amplification bandwidth in the spatial-frequency domain. This region has a shape of either a disk of radius $\sim x_0$, or an annulus of thickness $\sim x_0$, both centered at the symmetry axis. The occurrence of one or another case is controlled by the phase mismatch δ_0 in the propagation direction for the OPA [5], and by the cavity detuning parameter in the OPO case [6]. Figure 3 plots the amplification factor $|\overline{u}(|\vec{x}|, \Omega = 0)|^2$ for two values of δ_0, in the OPA case. The ratio of the amplification area to the resolution area S_R determines the number N of image elements that can be effectively amplified by the scheme. This number is assessed by

$$N = \frac{1}{(2\pi)^2} S_A \Delta k^2 ; \tag{7}$$

in the following we assume that $N \gg 1$.

We make several assumptions about the input image: (i) the field in the input plane P_1 is weak with respect to the pump, stationary in time, and in a coherent state, such that

$$\langle a_1(\vec{x}, \Omega)\rangle = \sqrt{2\pi}\, \delta(\Omega) \alpha_{\text{in}}(\vec{x}) , \tag{8}$$

where $|\alpha_{\text{in}}(\vec{x})|^2$ represents the mean number of photons per unit area and unit time; (ii) the input image is confined to (say) the upper half plane [$\alpha_{\text{in}}(\vec{x}) = 0$ for $y < 0$], and to the effectively amplified region; and (iii) variations of $\alpha_{\text{in}}(\vec{x})$ over regions of the order S_R are negligible. It follows that the stationary intensity distribution in the output plane P_4 is given by

$$\begin{aligned}\langle a_4^\dagger(\vec{x}, t) a_4(\vec{x}, t)\rangle = {} & |\overline{u}(|\vec{x}|, 0)|^2 \, |\alpha_{\text{in}}(-\vec{x})|^2 \\ & + |\overline{v}(|\vec{x}|, 0)|^2 \, |\alpha_{\text{in}}(\vec{x})|^2 \\ & + \frac{1}{S_R} \int \frac{d\Omega}{2\pi} \, |\overline{v}(|\vec{x}|, \Omega)|^2 . \end{aligned} \tag{9}$$

Here the first term is localized in the lower half plane $y < 0$, and corresponds to the amplified input image (signal image); the second contribution, in the upper half plane, corresponds to the phase-conjugate (idler) image (symmetrical parts of these images have the same intensity in the limit $|v| \gg 1$); while the last term is a pure noise contribution arising from spontaneous parametric down-conversion. The main purpose of introducing the finite-size pupil in our scheme is for evaluation of this noise term which diverges for $S_A \to \infty$ (see [6]).

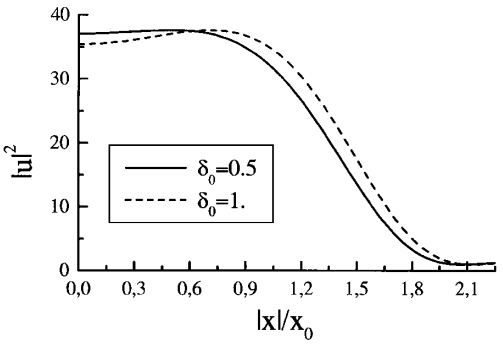

FIG. 3. OPA gain curves for two different values of the collinear phase mismatch δ_0.

Let us now consider two detectors 1 and 2 with quantum efficiency η that detect photons crossing two symmetrical regions of the signal image (1) and of the idler image (2) (Fig. 1). Operators $i_1(t)$, $i_2(t)$ represent the photocurrents produced in detectors 1, 2; their mean values are proportional to the mean photon fluxes:

$$\langle i_j(t)\rangle = \eta \int_{R_j} d\vec{x} \, \langle a_4^\dagger(\vec{x}, t) a_4(\vec{x}, t)\rangle \qquad (j = 1, 2) , \tag{10}$$

where the detection regions R_j are assumed larger than S_R. As for fluctuations, we evaluate the photocurrent noise spectra:

$$V_{jk}(\Omega) = \int_{-\infty}^{\infty} dt \, e^{i\Omega t} \langle \delta i_j(t) \delta i_k(0)\rangle \qquad (j, k = 1, 2) , \tag{11}$$

where $\delta i_j(t) = i_j(t) - \langle i_j(t)\rangle$. On the basis of our assumptions we obtain the following results:

$$V_{11}(0) = (SN)_1 + \eta^2 \int_{R_2} d\vec{x} \left\{ 2|\overline{u}(|\vec{x}|, 0)|^2 \, |\overline{v}(|\vec{x}|, 0)|^2 \, |\alpha_{\text{in}}(\vec{x})|^2 + \frac{1}{S_R} \int \frac{d\Omega}{2\pi} \, |\overline{v}(|\vec{x}|, \Omega)|^4 \right\} , \tag{12}$$

$$V_{12}(0) = \eta^2 \int_{R_2} d\vec{x} \left\{ 2|\overline{u}(|\vec{x}|, 0)|^2 \, |\overline{v}(|\vec{x}|, 0)|^2 \, |\alpha_{\text{in}}(\vec{x})|^2 + \frac{1}{S_R} \int \frac{d\Omega}{2\pi} \, |\overline{u}(|\vec{x}|, \Omega)|^2 \, |\overline{v}(|\vec{x}|, \Omega)|^2 \right\} , \tag{13}$$

where $(SN)_1 = \langle i_1(t)\rangle$ is the shot-noise contribution. $V_{22}(0)$ is obtained from $V_{11}(0)$ by replacing the index 1 by 2, and the function $|\overline{u}(x, 0)|^2$ by $|\overline{v}(x, 0)|^2$. For large amplification, $|v|^2 \gg 1$, fluctuations in regions 1 and 2 are very much above the shot-noise level. However, fluctuations in symmetrical portions of the two images are strongly correlated. The degree of correlation can be expressed through the fluctuation spectrum of the photocurrent difference $i_-(t) = i_1(t) - i_2(t)$:

$$V_-(\Omega = 0) = \int_{-\infty}^{\infty} dt \, \langle \delta i_-(t) \delta i_-(0)\rangle \tag{14}$$

$$= (SN)_- \left[(1 - \eta) + \eta \frac{(SN)_{\text{in}}}{(SN)_-} \right] , \tag{15}$$

where

$$(SN)_- = \langle i_1\rangle + \langle i_2\rangle , \tag{16}$$

$$(SN)_{\rm in} = \eta \int_{R_2} d\vec{x}\, |a_{\rm in}(\vec{x})|^2 \qquad (17)$$

are the shot noise for V_-, and for the portion R_2 of the input image, respectively. For large amplification and reasonably large detector efficiency the noise of the photocurrent difference is well below the shot-noise level, because $(SN)_{\rm in} \ll (SN)_-$. The effect is spectacular in the case of ideal detectors, $\eta = 1$, when $V_- = (SN)_{\rm in}$, and persists over all the frequency bandwidth T_a^{-1} of the amplifier. Hence quantum fluctuations in each output image are quite above the shot-noise level, but very well synchronized over a time scale $\gtrsim T_a$.

The fact that the system is fully in the quantum domain is confirmed by the conditional variance $V(i_1|i_2)$ [12] which describes how much the photocurrent fluctuations in R_1 (signal) can be reduced by measuring the fluctuations in R_2 (idler), and introducing a feedback loop. For $\eta|\overline{v}|^2 \gg 1$, assuming detection regions much smaller than the spatial scale of variation x_0 of the gain function $|\overline{v}|$, and neglecting the contributions from spontaneous parametric down-conversion, we arrive at

$$V(i_1|i_2) = V_{11}(0)\left[1 - \frac{V_{12}^2(0)}{V_{11}(0)V_{22}(0)}\right] \qquad (18)$$

$$\simeq (SN)_1\left[2(1-\eta) + \frac{2\eta - 1}{2\eta}\,\frac{1}{|\overline{v}(\Omega = 0)|^2}\right]. \qquad (19)$$

Clearly $V(i_1|i_2) < (SN)_1$ when $\eta > 1/2$, and in the limit $\eta = 1$ the ratio $V(i_1|i_2)/(SN)_1$ scales as $|\overline{v}|^{-2}$. In the same limit in which Eq. (19) is obtained, the expression (12) reduces to $V_{11}(0) \simeq (SN)_1\,(1 + 2\eta|\overline{v}(\Omega = 0)|^2)$. Hence, for $\eta = 1$ there is a drastic noise reduction by a factor $4|\overline{v}|^4$ when passing from the unconditioned variance V_{11} to the conditional variance $V(i_1|i_2)$.

Equation (15) shows that the noise reduction in the intensity difference is limited only by the noise in the input image. Of special interest is the case in which no image is injected, i.e., $\alpha_{\rm in} = 0$. In this case, for $\eta = 1$, $V_-(0) = 0$ and $V(i_1|i_2) = 0$. This represents a much sharper result than that obtained for an OPO with spherical mirrors [3].

Apart from Eq. (19), we took fully into account the contribution of the spontaneous down conversion; the condition for neglecting the noise term in Eq. (9) is rather compelling and can be estimated by replacing $\int d\Omega\, |\overline{v}(|\vec{x}|, \Omega)|^2$ by $|\overline{v}(|\vec{x}|, 0)|^2\, T_a^{-1}$. This gives

$$2\pi|\alpha_{\rm in}(\vec{x})|^2 S_R T_a \gg 1\,. \qquad (20)$$

The same inequality ensures that we can neglect the terms independent of $|\alpha_{\rm in}(\vec{x})|^2$ in Eqs. (12) and (13). For an OPA, using the experimental setup in [13] as a guideline, we take the values $\lambda = 10^{-4}$ cm, $f = 100$ cm, $l_{\rm eff} = 1.2$ cm, $S_A^{1/2} = 1$ cm, which gives $S_R^{1/2} = 8.3 \times 10^{-3}$ cm, and $N \approx 2300$ amplified image elements. For an input image intensity of 10 W/cm^2 [14], and $2\pi T_a = 10^{-13}$ s, the left-hand side of Eq. (20) is on the order of 10^2. In the OPO case, using a self-imaging resonator [15], a value of $l_{\rm eff}$ similar to that of the OPA can be attained, so we can consider the same parameter values. Since in this case $T_a \sim 10^{-8}$ s, condition (20) can be fulfilled with cw operation.

From these estimations we can conclude that experimental observation of the phenomenon that we describe in this paper appears compatible with present experiments on parametric down-conversion and amplification [8,13], and on single-pass parametric amplification of optical images [16]. The results of our analysis are quite general and hold for an OPO, for an OPA with generic dispersion law, and also for the four-wave mixing processes, because the input-output relations are given by a unitary transformation of the same form [17].

This work was supported by the Network QSTRUCT of the TMR Programme of the EU, and by the MURST project "Spatial Pattern Control in Sistemi Ottici Nonlineari."

[1] P. G. Kwiat, K. Mattle, H. Weinfurter, A. Zeilinger, A. V. Sergienko, and Y. H. Shih, Phys. Rev. Lett. **75**, 4337 (1995).
[2] L. A. Lugiato, M. Brambilla, and A. Gatti, in "Advances in Atomic, Molecular and Optical Physics," edited by B. Bederson and H. Walther (Academic Press, Boston, 1998), Vol. 40, pp. 229ff.
[3] I. Marzoli, A. Gatti, and L. A. Lugiato, Phys. Rev. Lett. **78**, 2092 (1997).
[4] For the OPO one should consider, more precisely, a ring cavity with one input/output mirror; see Fig. 1 of [6].
[5] M. I. Kolobov and I. V. Sokolov, Sov. Phys. JETP **69**, 1097 (1989); Phys. Lett. A **140**, 101 (1989).
[6] M. I. Kolobov and L. A. Lugiato, Phys. Rev A **52**, 4930 (1995).
[7] C. M. Caves and B. L. Schumaker, Phys. Rev. A **31**, 3068 (1985).
[8] M. L. Marable, S.-K. Choi, and P. Kumar, Opt. Expr. **2**, 84 (1998).
[9] O. Aytür and P. Kumar, Phys. Rev. Lett. **65**, 1551 (1990).
[10] J. A. Levenson, I. Abram, T. Rivera, P. Fayolle, J. C. Garreau, and Ph. Grangier, Phys. Rev. Lett. **70**, 267 (1993).
[11] A similar situation arises when considering a finite-size pump beam instead of a plane wave.
[12] Ph. Grangier, Phys. Rep. **219**, 121 (1992).
[13] A. Gatti, L. A. Lugiato, G-L. Oppo, R. Martin, P. DiTrapani, and A. Berzanskis, Opt. Expr. **1**, 21 (1997).
[14] This would require pulsed operation, but our treatment remains valid, provided the time duration of the pulse is much longer than T_a.
[15] J. A. Arnaud, Appl. Opt. **8**, 189 (1969).
[16] F. Devaux and E. Lantz, J. Opt. Soc. Am. B **12**, 2245 (1995); F. Devaux and E. Lantz (to be published).
[17] P. Kumar and M. I. Kolobov, Opt. Commun. **104**, 374 (1994); A. V. Belinskii and N. N. Rosanov, Opt. Spektrosk. **73**, 153 (1992) [Opt. Spectrosc. (USSR) **73**, 89 (1992)].